3^{rd} *Int. Symposium on Turbulence Heat and Mass Transfer, pp. 381-388*
Y. Nagano, K. Hanjalić and T. Tsuji (Editors)

Comparison of Near-wall Behavior and its Effect on Heat Transfer for $k-\omega$ and $k-\varepsilon$ Turbulence Models in Rib-roughened 2D Channels

J. Bredberg[1], L. Davidson[1], and H. Iacovides[2]

[1]*Department of Thermo and Fluid Dynamics, Chalmers University of Technology, S-412 96 Gothenburg, Sweden*

[2]*Department of Mechanical Engineering, UMIST, P.O. Box 88, Manchester, M60 1QD, UK*

Abstract — The connection between flowfield and heat transfer predictions with two-equation models in a 2D rib roughened channel is studied. Using the standard constant Prandtl number heat transfer model, the necessity of accurately predicting the wall friction in order to achieve reasonable heat transfer predictions is shown. The near-wall behavior of three different but commonly used two-equation models is included and its influence on the heat transfer is discussed. It was found that the Reynolds number dependency on the Nusselt number for all models is too strong, and that the two-layer or zonal model is inadequate for heat transfer predictions in these flow configurations.

1. Introduction

It has been observed in previous papers that the near-wall behavior of turbulence models is crucial for the accurate prediction of heat transfer. This paper evaluates the near-wall performance of three different two-equation models in a 2D rib-roughened channel. The rib-roughened channel is an inherent structure of a gas-turbine blade where the ribs are used to break up the internal coolant flow and increase the turbulence and hence the heat transfer. The geometry configuration of the channel is shown in Fig. 1, where, P/e, is the rib-pitch to rib-height ratio and, H/e, is the channel-height to rib-height ratio. The turbulence models used in this study are the $k-\varepsilon$ of Launder and Sharma [1] with the Yap-correction [2] (denoted $k-\varepsilon$ in the figures), the $k-\omega$ of Abid *et al.* [3] ($k-\omega$) and the two-layer or zonal $k-\varepsilon$ of Chen and Patel [4] (zonal). The accurate prediction of the Launder-Sharma model has been noted in Iacovides and Raisee [5], while the benefit of the specific dissipation rate based $k-\omega$ has been shown in Bredberg and Davidson [6] and Bredberg [7] in these configurations. In this paper the connection between prediction of the flowfield and heat transfer, using a constant turbulent Prandtl number heat transfer model, is discussed.

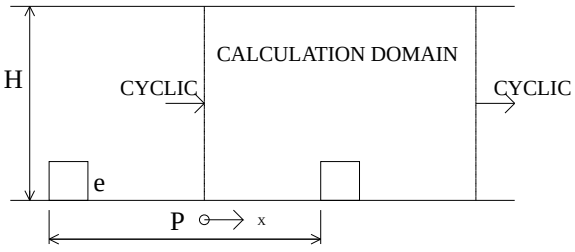

Re	100 000	40 000
P/e	10	10
H/e	10	10
Exp. Data	[8]	[8]

Figure 1: Data for the test cases

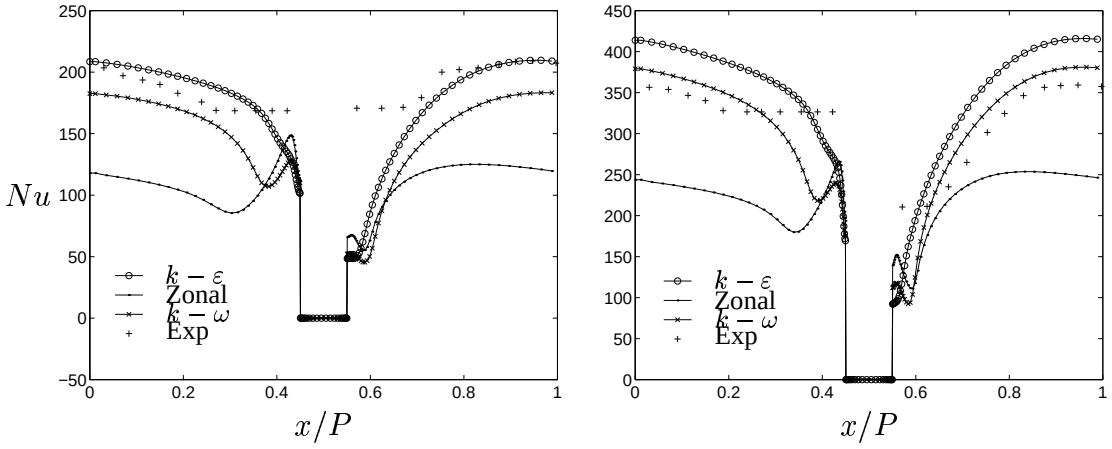

(a) $Re_H = 40\,000$ (b) $Re_H = 100\,000$

Figure 2: Nusselt number, lower wall

2. Results and Discussion

Two different experiments done by Nicklin [8] are used as comparisons in this paper. The Reynolds number based on the channel height and mean velocity were: $Re_H = 40\,000$ and $Re_H = 100\,000$. The measured quantity was the heat transfer, which can be non-dimensionalized to yield the Nusselt number:

$$Nu = \frac{2q_w PrH}{\mu c_p (T_w - T_{bulk})} \tag{1}$$

Heaters with a constant heat-flux were attached to both the lower and upper wall, with the rib itself thermally insulated. In the predictions, the same mesh was used for both cases and consisted of 112×122 grid nodes, see [7] for mesh comparisons.

The Nusselt number along the lower wall depicted in Fig. 1, is shown in Fig. 2. Table 1 compares the predictions obtained by the different turbulence models with the experiment at the specific point of $x/P = 0$. The Table together with Fig. 2 clearly indicates too strong an effect of the Reynolds number on the Nusselt number for all models.

	Experiment	$k-\varepsilon$	Zonal	$k-\omega$
Nu(100):	357	414	244	377
Ratio Pred/Exp:	-	1.16	0.68	1.06
Nu(40):	204	209	118	183
Ratio Pred/Exp:	-	1.02	0.58	0.90
Ratio(100/40):	1.75	2.0	2.1	2.1

Table 1: Nusselt number, lower wall

For fully developed pipe flow, the Nusselt number dependency on the Reynolds number and Prandtl number has been compiled into the Dittus-Boelter relation, as given by McAdams [9]:

$$Nu = 0.023 Re^{0.8} Pr^{0.4} \tag{2}$$

The ratio of the Reynolds number raised to 0.8 gives a factor of 2.1 in favor of the higher Reynolds number, which is approximately what was found from the predictions. The experimental data however give a ratio of 1.75 in the mid-range between the ribs. This is equivalent to $Nu \sim Re^{0.6}$, which is close to the value of $2/3$ found by Richardson [10] and Sogin [11] in their studies of heat transfer for separated flow around bluff-bodies.

As reported by Chieng and Launder [12], the Launder-Sharma $k-\varepsilon$ model severely over predicts the near-wall length-scale, and hence the Nusselt number. Yap re-examined the data and added a length-scale modification to the dissipation rate equation, the Yap-correction, which improves the heat transfer predictions, see also Launder [13]. The above Yap-corrected $k-\varepsilon$ model predicts the low Reynolds number case accurately, although it over predicts the high Reynolds number case. Thus it seems that the Yap-correction does not sufficiently reduce the Reynolds number dependency, at least in these flow conditions. Apart from this, the overall profile is accurately captured.

In the case of the Chen and Patel zonal $k-\varepsilon$ model, the overall profile shows less agreement, especially upstream of the rib, where there is a relatively large increase in Nusselt number prior to the rib, contrary to what was found in the experiments. In addition, the overall level of the Nusselt number is severely under predicted in both cases. This is also consistent with the results of Iacovides *et al.* [5], [14] in similar cases, although with slightly different constants in the model. The zonal model yields a rather flat profile in the mid-interval between the ribs, with a local maximum Nusselt number too close to the rib. The predicted overall maximum Nusselt number is found immediately upstream of the rib, which is clearly erroneous when compared with the measured data.

The Abid *et al.* $k-\omega$ model agrees well with the experiments, although the strong Reynolds dependency makes the model over predict the heat transfer for even higher Reynolds number, see [6], [7]. The largest deviation from the measured data is found downstream of the rib, where the model predicts too large a drop in the Nusselt number. The discrepancy is somewhat less in the $Re_H = 100\,000$ case. There is also a drop in the Nusselt number in the upstream region of the rib, with an increase immediately in front of the rib. This variation in Nusselt number is not visible at all from the measurements.

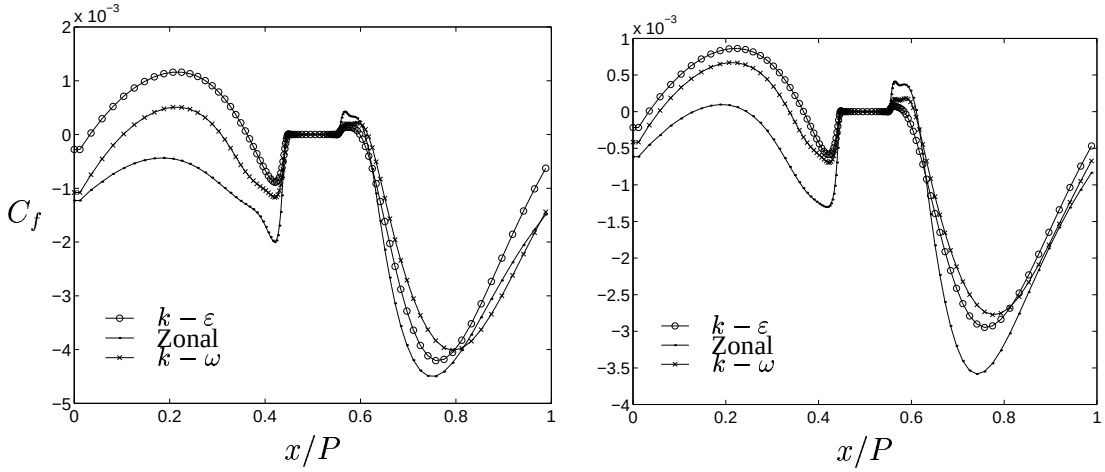

(a) $Re_H = 40\,000$ (b) $Re_H = 100\,000$

Figure 3: Friction coefficient, lower wall

It can be argued that there is a strong connection between the flowfield and heat transfer, which can be exemplified with the Reynolds analogy; $Nu = RePrC_f/2$, where the friction coefficient, is defined as $C_f = \tau_w/\rho U_b^2/2$. Note that this relation is only valid when the pressure gradient could be neglected and also where identical thermal and flowfield boundary conditions applies, and hence not in this situation. Although the above limitation and additionally that there are no measured data of friction coefficient available, it is still interesting to compare the predicted C_f and Nu for the different models. The friction coefficient along the lower wall is shown in Fig. 3 and should be compared with the Nusselt number in Fig. 2.

Both the $k-\varepsilon$ and the $k-\omega$ yield similar profiles where the $k-\varepsilon$ generally predicts a higher friction coefficient, which is consistent with the Nusselt number comparisons. The only part where the $k-\omega$ returns higher C_f-values is closely upstream of the rib, where it also has an erroneous variation in the Nusselt number. The differences decrease for the higher Reynolds number case. Fig. 3 also clearly illustrates the separation and reattachment points - indicated by zero friction coefficient - with the $k-\omega$ model giving a longer recirculation bubble than the $k-\varepsilon$, especially in the $Re = 40\,000$ case.

Comparing these results with those of the zonal model reveals the fundamental difference between the models. In the zonal model, the near-wall length-scale is set using the wall distance. This has, as is obvious from Fig. 3, a strong influence on the location of the reattachment points, which in the lower Reynolds number case vanishes altogether. In the higher Reynolds number case the model returns only a very short reattached flow in between the ribs. Turbulence is generated through shearing in the flow and is particularly strong around reattachment points. In the case of the zonal model, which either doesn't predict or predicts a very weak reattachment, less turbulence is produced with a lower predicted Nusselt number as a result, see also the discussion below.

Switching to the upper wall, the differences between the turbulence models are very slight, as is apparent in Fig. 4.

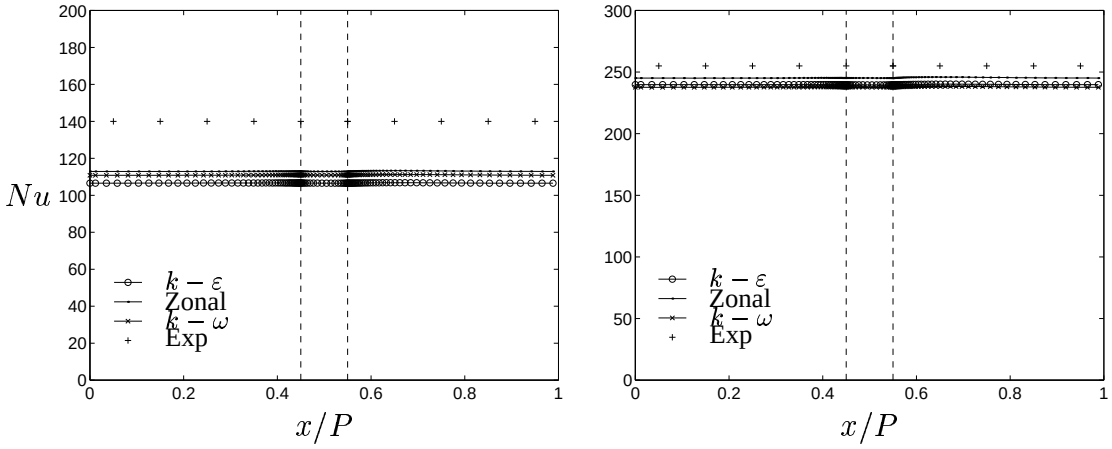

(a) $Re_H = 40\,000$ (b) $Re_H = 100\,000$

Figure 4: Nusselt number, upper wall

The data for the upper wall at the point $x/P = 0$ are compiled in Table 2. The three turbulence models under predict the heat transfer on the upper wall by approximately 20% in the $Re = 40\,000$ case, with closer agreement, though still under predicting in the $Re = 100\,000$ case.

	Experiment	$k-\varepsilon$	Zonal	$k-\omega$
Nu(100):	255	240	245	235
Ratio Pred/Exp:	-	0.94	0.96	0.92
Nu(40):	140	107	114	111
Ratio Pred/Exp:	-	0.76	0.81	0.79
Ratio(100/40):	1.82	2.24	2.15	2.12

Table 2: Nusselt number, upper wall

What is however more interesting is the relatively high value of the Nusselt number on the upper wall for the zonal model, especially in the $Re = 100\,000$ case. Comparing Figs 4 and 2, it is seen that the zonal model predicts similar levels of the Nusselt number on both the ribbed and non-ribbed wall. This can be explained by the fact that the zonal model imposes the same length-scale distribution on both walls, disregarding any recirculational motions of the fbw. Thus, the high Nusselt number on the upper wall is an effect of the general increase in turbulence in the channel and is not caused by any local effect, see also below. Note also that the relatively low Nusselt number on the lower wall is explained by the fact that the zonal model remains separated over the entire rib-interval, see Fig. 3.

	Experiment	DB	$k-\varepsilon$	Zonal	$k-\omega$
Nu(100):	187	199	182	171	161
Ratio Pred/Exp:	-	1.06	0.97	0.86	0.81
Nu(40):	95	96	81	84	78
Ratio Pred/Exp:	-	1.01	0.85	0.88	0.82
Ratio(100/40):	1.97	2.07	2.25	2.04	2.06

Table 3: Nusselt number, smooth channel

As a reference, the turbulence models were also used to predict the Nusselt number in a smooth channel. The computed values are compared in Table 3 with the calculated Nusselt number using the Dittus-Boelter (DB) equation and experimental values by Kays and Leung [15]. All models under predict in both cases. The relative large under prediction by the $k-\omega$ model in the smooth channel is associated with the fact that the standard $k-\omega$ models yield too low a value of the turbulent kinetic energy in the near-wall region, and hence too low a heat transfer.

Tables 2 and 3 illustrate the influence of the lower ribbed wall on the upper smooth wall. The predicted increase in Nusselt number, as a result of the opposite ribbed wall, is between 32% and 46% for the higher Reynolds number case and between 32% and 42% for the lower Reynolds number case, with higher values for the $k-\omega$ model, and lower for the $k-\varepsilon$ model.

The experimental data give an increase of 28% and 46%, for the two Reynolds numbers, compared with the DB equation, and hence deviate from the pre-assumed relation, $Nu \sim Re^{0.8}$. The actual exponent is closer to the previously reported value of $2/3$. Note that this lower exponent is not caused by any mean fbw effects but is rather an indication of the general increase of turbulence in the fbw, which is augmented due to the periodically repeated turbulence generating ribs on the lower wall.

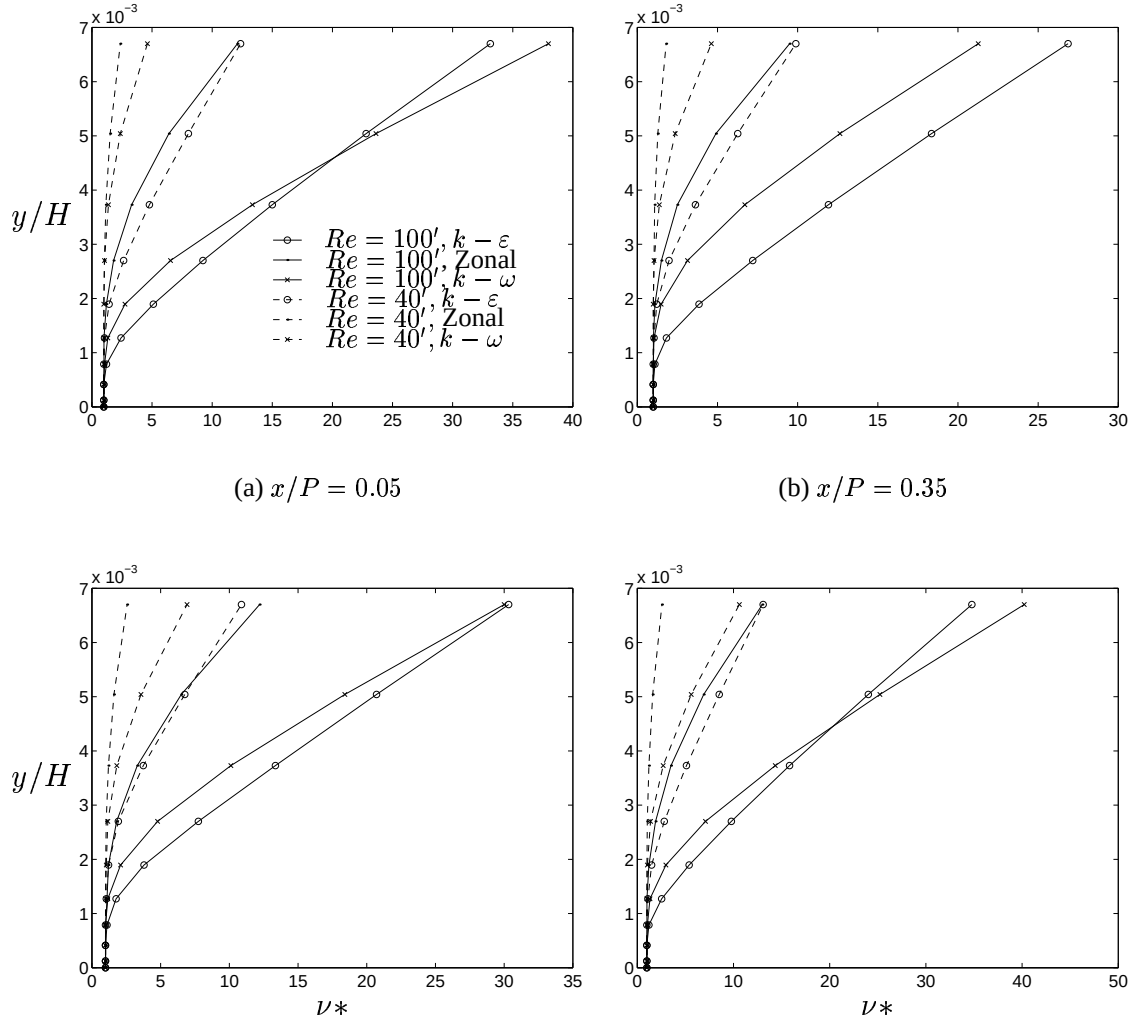

(a) $x/P = 0.05$ (b) $x/P = 0.35$

(c) $x/P = 0.75$ (d) $x/P = 0.95$

Figure 5: Near-wall viscosity, lower wall, markers indicate cell node locations.

The differences in the predicted Nusselt number may be discussed in relation to several specifi c detailed near-wall data, where here the total viscosity, ν, and the turbulent kinetic energy, k, were chosen. The viscosity is, through the heat transfer model, the parameter that affects the Nusselt number the most. The turbulent kinetic energy was selected since this is the one turbulent parameter that is common for the models.

The total viscosity profi les normalized with the molecular viscosity, according to: $\nu* = (\nu + \nu_t)/\nu$, are plotted in Fig. 5. The normalized viscosity is one at the wall, indicating zero turbulent viscosity. There is obviously a large difference between the high and low Reynolds number cases, where the higher Reynolds case generates more turbulent viscosity, owing to the larger turbulence production. The highest levels of viscosity (and k) occur in the recirculation bubble upstream of the reattachment point, see Figs 5(a) and 5(d) and Figs 6(a) and 6(d).

The $k - \varepsilon$ generally yields the highest levels of viscosity, while the zonal the lowest, at both Reynolds numbers. This has a direct influence on the predicted Nusselt number through the heat transfer model, and hence the $k - \varepsilon$ model returns the highest predicted Nu and the zonal

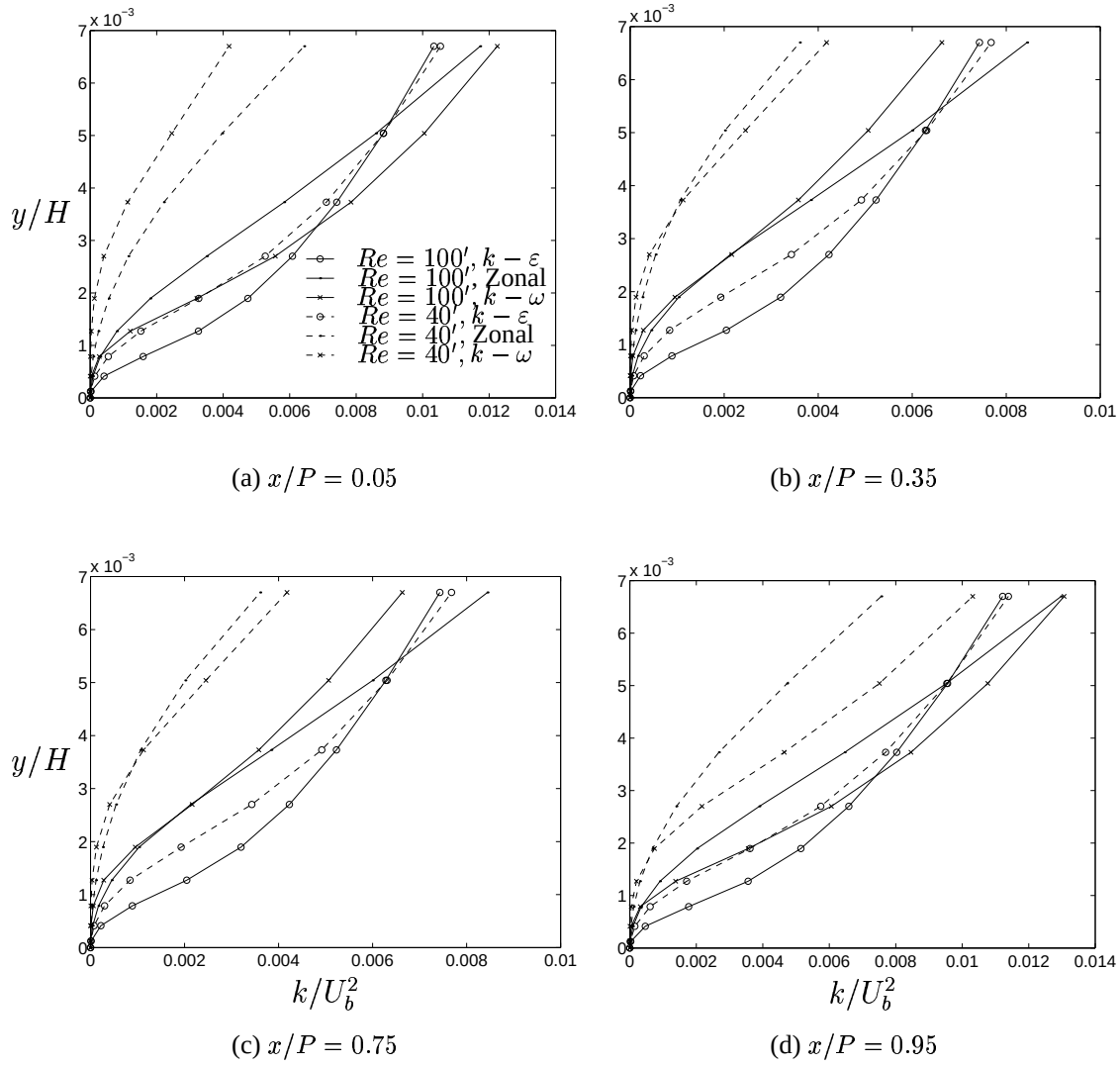

(a) $x/P = 0.05$ (b) $x/P = 0.35$

(c) $x/P = 0.75$ (d) $x/P = 0.95$

Figure 6: Near-wall turbulent kinetic energy, lower wall, markers indicate cell node locations.

the lowest. To find the rationale for this, attention is given to the turbulent quantity.

The normalized turbulent kinetic energy is plotted in Fig. 6. There is no distinct difference between the models apart from the fact that the $k-\varepsilon$ produces quite a high k even in the low Reynolds number case. From this it can be concluded that the main difference and also discrepancies among the models are their representation of the length-scale. Notably, the turbulent viscosity is identically defined for all three models, $\mu_t = C_\mu \sqrt{k} l$, where l is the length-scale represented either by $\omega = \sqrt{k}/l$ or by $\varepsilon = k^{3/2}/l$. Thus, with a similar k-profile, the difference is a direct consequence of either over or under estimation of the length-scale. In the case of the zonal model, the length-scale is clearly under predicted while, for a non-Yap-corrected $k-\varepsilon$, it is severely over predicted, [12]. A notable difference between the $k-\varepsilon$ and $k-\omega$ model is their profiles of the turbulent kinetic energy, where $k-\varepsilon$ returns a higher value of k in the immediate near-wall area, whereas $k-\omega$ gradually increases the turbulent kinetic energy to higher values in the outer near-wall region, $y/H > 0.005$. This is most likely a consequence of the length-scale representation, for which the $k-\omega$ yields very small values close to the wall owing to the infinite value of the specific dissipation rate, ω, at the wall.

3. Conclusions

- The appropriate Reynolds dependency of the Nusselt is re-confi rmed to be less in separated fbws than in equilibrium fbws.
- The turbulence models evaluated have too strong a Reynolds number dependency on the Nusselt number in recirculating fbws.
- The $k-\omega$ and $k-\varepsilon$ models both predict reasonable heat transfer.
- The zonal model is inadequate for heat transfer predictions in rib-roughened channels through its faulty turbulent length-scale representation.

Acknowledgments

The present work was supported by the Swedish Gas Turbine Center. The author, Bredberg would also like to express his appreciation for the support by the colleagues at UMIST, UK.

References

1. B.E. Launder and B.I. Sharma. Application of the energy-dissipation model of turbulence to the calculation of flow near a spinning disc. *Letters in Heat and Mass Transfer*, 1:131–138, 1974.
2. C.R. Yap. *Turbulent heat and momentum transfer in recirculation and impinging flows*. PhD thesis, Dept. of Mech. Eng., Faculty of Technology, Univ. of Manchester, 1987.
3. R. Abid, C. Rumsey, and T. Gatski. Prediction of nonequilibrium turbulent flows with explicit algebraic stress models. *AIAA Journal*, 33:2026–2031, 1995.
4. H.C. Chen and V.C. Patel. Near-wall turbulence models for complex flows including separation. *AIAA Journal*, 26:641–649, 1988.
5. H. Iacovides and M. Raisee. Computation of flow and heat transfer in 2-D rib roughened passages. In K. Hanjalić and T.W.J. Peeters, editors, *2nd Int. Symp. on Turbulence Heat and Mass Transfer (Addendum)*, pages 21–30, Delft, 1997. Delft University Press.
6. J. Bredberg and L. Davidson. Prediction of flow and heat transfer in a stationary 2-D rib roughened passage using low-Re turbulent models. In *3:rd European Conference on Turbomachinery*, pages 963–972. IMechE, 1999.
7. J. Bredberg. Prediction of flow and heat transfer inside turbine blades using EARSM, $k-\varepsilon$ and $k-\omega$ turbulence models. Report, Department of Thermo and Fluid Dynamics, Chalmers University of Technology, Gothenburg, 1999. Also available at www.tfd.chalmers.se/˜bredberg.
8. G. J. E. Nicklin. Augmented heat transfer in a square channel with asymmetrical turbulence promotion. Final year project report, Dept. of Mech. Eng., UMIST, Manchester, 1998.
9. W.H. McAdams. *Heat Transmission*. McGraw-Hill, New York, 2nd edition, 1942.
10. P.D. Richardson. Heat and mass transfer in turbulent separated flows. *Chemical Eng. Sci*, 18:149–155, 1963.
11. H.H. Sogin. A summary of experiments on local heat transfer from the rear of bluff obstacles to a low speed airstream. *Trans AMSE*, 86:200–202, 1964.
12. C.C. Chieng and B.E. Launder. On the calculation of turbulent heat transfer transport downstream an abrupt pipe expansion. *Num Heat Transfer*, 3:189–207, 1980.
13. B.E. Launder. On the computation of covective heat transfer in complex turbulent flows. *J. Heat Transfer*, 110:1112–1128, 1988.
14. H. Iacovides. Computation of flow and heat transfer through rotating ribbed passages. In *11th Symposium on Turbulent Shear Flows*, 1997.
15. W.M. Kays and E.Y. Leung. Heat transfer in annular passages - hydrodynamically developed turbulent flow with arbitrarily prescribed heat flux. *Int J of Heat and Mass Transfer*, 6:537–557, 1963.